LETTERS
PUBLISHED ONLINE: 5 JULY 2009 | DOI: 10.1038/NMAT2494
nature materials

Organic electronics for precise delivery of neurotransmitters to modulate mammalian sensory function

Daniel T. Simon[1,2], Sindhulakshmi Kurup[2,3], Karin C. Larsson[2,3], Ryusuke Hori[4]*, Klas Tybrandt[1,2], Michel Goiny[4], Edwin W. H. Jager[1,2], Magnus Berggren[1,2], Barbara Canlon[4] and Agneta Richter-Dahlfors[2,3]†

Significant advances have been made in the understanding of the pathophysiology, molecular targets and therapies for the treatment of a variety of nervous-system disorders. Particular therapies involve electrical sensing and stimulation of neural activity[1–4], and significant effort has therefore been devoted to the refinement of neural electrodes[5–8]. However, direct electrical interfacing suffers from some inherent problems, such as the inability to discriminate amongst cell types. Thus, there is a need for novel devices to specifically interface nerve cells. Here, we demonstrate an organic electronic device capable of precisely delivering neurotransmitters *in vitro* and *in vivo*. In converting electronic addressing into delivery of neurotransmitters, the device mimics the nerve synapse. Using the peripheral auditory system, we show that out of a diverse population of cells, the device can selectively stimulate nerve cells responding to a specific neurotransmitter. This is achieved by precise electronic control of electrophoretic migration through a polymer film. This mechanism provides several sought-after features for regulation of cell signalling: exact dosage determination through electrochemical relationships, minimally disruptive delivery due to lack of fluid flow, and on–off switching. This technology has great potential as a therapeutic platform and could help accelerate the development of therapeutic strategies for nervous-system disorders.

To develop a programmable 'machine-to-brain' communication platform, numerous criteria must be met, such as dosage precision and dynamic spatial and temporal control. Furthermore, delivery should preferably be achieved with minimal fluid flow, as liquid flow can lead to undesirable effects such as chemical gradient disruption[9] or increased pressure in compartments with limited volume. Non-convective delivery would enable the introduction of biological substances *per se* into small compartments in organs such as the cochlea. Organic conjugated polymers have been investigated in recent years as delivery platforms that fulfil many of these requirements, in part owing to their chemical and material properties that facilitate their incorporation into bio-medical devices[10,11]. As volume-change actuators, they have been explored as reversible valves exposing drug-loaded microreservoirs[12]. This electrochemical actuation has also been investigated for the release of drugs from the polymer itself[13,14]. Abidian *et al.* have even demonstrated controlled release from conducting polymer-coated drug-loaded nanofibres fabricated directly on a neural implant electrode[15].

Each of these technologies takes advantage of the role of ions in polymer conduction. Electronic and ionic conduction coexist—and are often coupled—in conducting polymer systems[16,17]. Indeed, the fact that electronic conduction can be ion mediated leads to the conclusion that these materials could provide an ideal interface for signal transduction between electron- and ion-mediated systems. This concept was recently demonstrated in an organic electronic 'ion pump'[18]. When addressing the device with a driving voltage, K^+ was electrophoretically transported from a source electrolyte, through a film of the conducting polymer[19] poly(3,4-ethylenedioxythiophene) doped with poly(styrenesulphonate) (PEDOT:PSS)[20–22], into a target reservoir containing neuronal cells. Local increase of extracellular [K^+] depolarized the cell membrane, thereby activating membrane-bound Ca^{2+} pumps; that is, the electronic input signals were translated into ion fluxes and, in turn, activation of intracellular signal transduction pathways.

This technology, based on simple monolithic design, realizes the criteria stated above. Delivery is achieved with minimal physiological disturbances, as electronic signals are translated into ion transport in the absence of fluid flow. Spatial control is defined by photolithographic patterning[18] (see Supplementary Information), whereas temporal control is achieved by modulation of the electrophoretic driving voltage. The latter provides the possibility of programming the ion transport to mimic dynamic temporal patterns, for example, the oscillations characteristic of Ca^{2+} signalling[23].

To analyse whether we could expand the repertoire of signal substances transported through the electronic matrix, we tested the neurotransmitters glutamate (Glu), aspartate (Asp) and γ-amino butyric acid (GABA). These small molecules exist as positively charged ions depending on the pH, which is required for the electrophoretic action of the ion pump. Glu is the principal excitatory neurotransmitter in the central nervous system (CNS), where it mediates fast synaptic transmission. Together with its receptors, Glu has critical roles in synaptic plasticity, basic processes of memory and learning, and brain development, as well as neurological and psychiatric disorders[24].

[1]Department of Science and Technology (ITN), Linköping University, S-601 74 Norrköping, Sweden, [2]Strategic Research Center for Organic Bioelectronics (OBOE), Linköping and Stockholm, Sweden, [3]Department of Neuroscience; [4]Department of Physiology and Pharmacology, Karolinska Institutet, S-171 77 Stockholm, Sweden. *Present address: Department of Otolaryngology, Head & Neck Surgery, Graduate School of Medicine, Kyoto University, Kyoto 606-8507, Japan. †e-mail: agneta.richter.dahlfors@ki.se.

Asp is also an excitatory neurotransmitter, whereas GABA is the principal inhibitory neurotransmitter in the mammalian CNS. The pathophysiology of numerous neuropsychiatric disorders, including anxiety and depression, is suggested to be due to disturbances in the GABA system[25].

We prepared planar ion pump devices, comprising a single, biocompatible PEDOT:PSS layer, as previously reported[18]. The single film is divided by an electronically insulating—but still ionically conducting—region (Fig. 1 and Supplementary Information). When voltage is applied, an electrochemical circuit is established, leading to oxidation of the source electrode (anode, equation (1)), and reduction of the target electrode (cathode, equation (2)), where M^+ is the cation present in the source electrolyte.

$$PEDOT^0 + M^+:PSS^- \rightarrow PEDOT^+:PSS^- + M^+ + e^- \quad (1)$$

$$PEDOT^+:PSS^- + M^+ + e^- \rightarrow PEDOT^0 + M^+:PSS^- \quad (2)$$

The cations are electrophoretically transported through the region of film joining the two electrodes, then enter the cathodic side of the film, where they are delivered into the electrolyte. This structure of electronically conducting electrodes separated by an electronically insulating channel enables application of a wide range of voltages—in excess of 30 V—without excessive electric fields in the target system. Furthermore, the use of PEDOT:PSS alleviates problems associated with secondary electrochemical reactions at such elevated voltages (see Supplementary Information).

Using Glu, Asp and GABA as source electrolytes, the delivery capabilities of the device were demonstrated at multiple driving voltages for a variety of times, with individual devices used for each parameter tested (Fig. 2a–c). By comparing the integrated electronic current to the quantity of neurotransmitters delivered into the target electrolyte (see Supplementary Information), a transport efficiency can be defined by the electron/molecule ratio. This ratio is precisely 2.7 ± 0.2 for Glu ($n = 16$), 6.3 ± 0.5 for Asp ($n = 10$) and 1.3 ± 0.1 for GABA ($n = 10$) (value $\pm$ s.d.). For materials with low pK_a, that is, Glu and Asp, the excess protons present in the source solution will also be pumped. Owing to the smaller size of protons compared with Glu or Asp, their mobility through the channel can be significantly higher, explaining the larger electron/molecule ratios for Glu and Asp. The transport rate can be tuned by the operating voltage, providing a full range of transport up to quantities of the order of 100 μM in the total liquid volume. Locally however, the concentration can be significantly higher before the molecules diffuse away[23]. The approximate concentration of Glu in the synaptic cleft has been reported to be 2–1,000 μM (ref. 26); thus, the device operates in a relevant physiological range.

The lifetime of the device is limited by the amount of oxidizable PEDOT (see equation (1)) and can thus be tailored by the electrode dimensions (see Supplementary Information). The present electrode geometry enables device operation of the order of 1 h in constant pumping mode, that is, constant current. The PEDOT could also be returned to a more reduced state, for example, by reversing the voltage. Using pulsed delivery[23], the lifetime should be bounded only by the concentration of molecules in the source electrolyte and could therefore be markedly extended. Figure 2d illustrates that the delivery rate is stable after an initial equilibration period corresponding to the time required to fill the channel with the intended ions on first use.

The successful transport of neurotransmitters encouraged us to redesign the device into an encapsulated, syringe-like form to enable its use *in vivo*. The first step in this development was the realization that the channel region could comprise an extra electrolyte (Fig. 1b). This geometry could enable the central electrolyte to become the effective target system, with the original target acting simply as the electrochemical cathode. By 'folding' this system, and providing encapsulation around the individual electrolytes, a syringe-like device is achieved (Fig. 1c,d). The operating principle is similar to the planar device, except that cations from the source are delivered to an external target electrolyte, and cations are extracted from this target region and drawn in towards the cathode system, completing the electrochemical circuit.

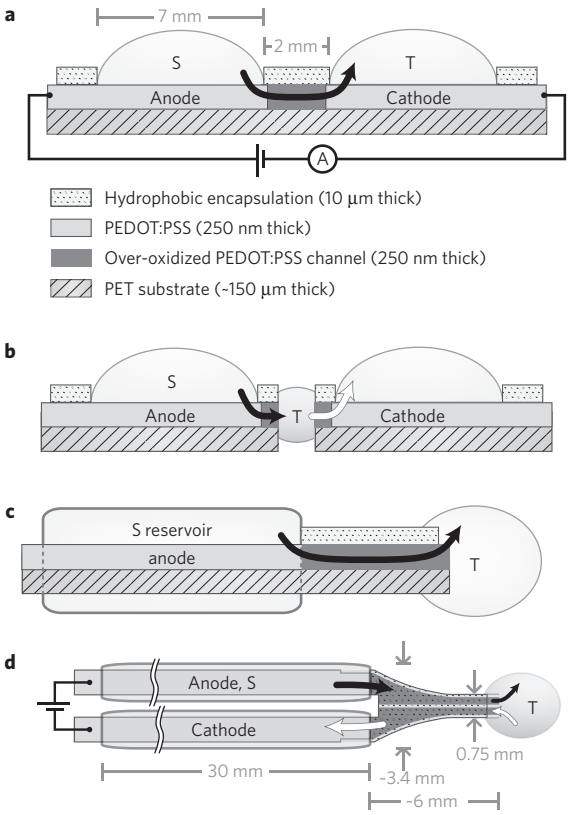

Figure 1 | Planar and encapsulated geometries of the delivery device. **a**, Side view of the planar device used in initial Glu, Asp and GABA transport studies. The black arrow indicates the flow of charged neurotransmitters from the source electrolyte, S, through the anode, then through the over-oxidized channel and finally out into the target electrolyte, T, through the cathode. Layer thicknesses are indicated in the material legend. **b**, Side view showing the developmental progression from the planar device (**a**), to the planar device with intermediate electrolyte (salt bridge)—that is, the effective target system T. The white arrow indicates the flow of arbitrary positively charged species from T into the cathodic electrolyte. **c**, Side-view scheme of the encapsulated device. Only the source/anode system is shown with cylindrical encapsulation. The arrow again indicates ion flow. **d**, Top view of the encapsulated device, showing both electrolyte chambers and the requisite target system T. The arrows are analogous to those in **b**. The electrolyte reservoir tubes are 2 mm in outer diameter.

To ascertain whether the encapsulated device can be used for cell stimulation similarly to the planar device[18], *in vitro* experiments were carried out. Astrocytes, a sub-type of glial cells present in the CNS, express the receptor for Glu. On binding of Glu, membrane-bound ion channels open immediately, promoting Ca^{2+} influx[27–29]. Therefore, astrocytes represent an ideal system to monitor Glu activation of cells using real-time single-cell ratiometric Ca^{2+} imaging. The device was loaded with Glu (source) and NaCl (cathodic) electrolytes and mounted with the tip in contact with the bottom of a dish, adjacent to primary murine astrocytes. After initial baseline recordings of intracellular Ca^{2+} with the delivery device in the off-state, Glu transport was activated. A significant increase

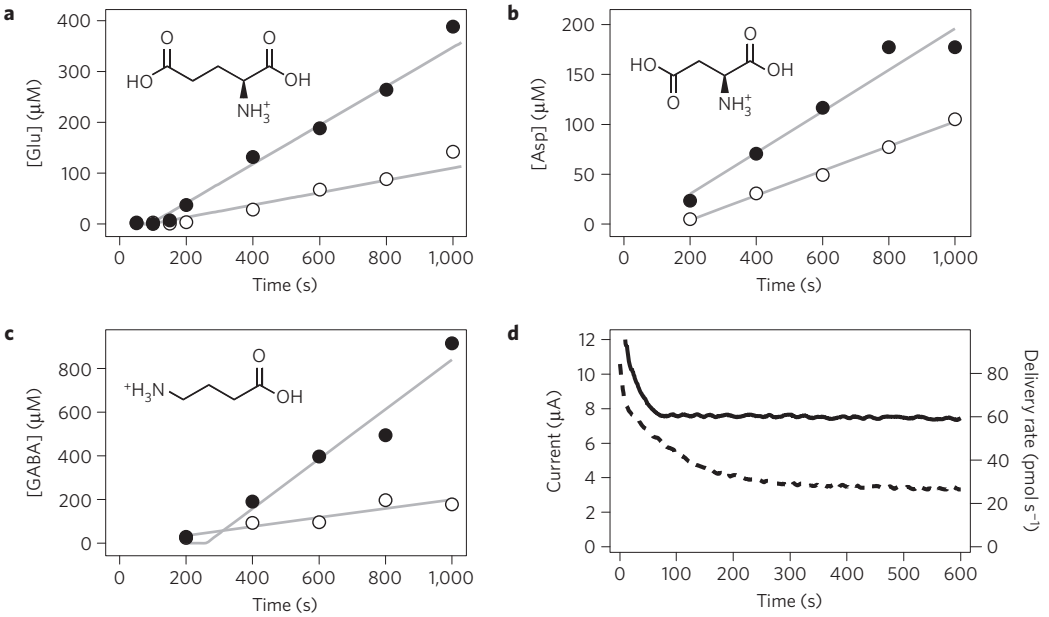

Figure 2 | Transport of neurotransmitters in the planar delivery device. a–c, Concentration of Glu (148 g mol^{-1}) (**a**), Asp (134 g mol^{-1}) (**b**) and GABA (104 g mol^{-1}) (**c**) in the target electrolyte (150 μl) as a function of time, where the device was operated at 4 V (open symbols) and 8 V (filled symbols). The grey lines are linear fits with non-zero time offset (see Supplementary Information). The insets show the chemical structures of the materials in their positively charged form. **d**, Representative current versus time data at 4 V (dashed line) and 8 V (solid line) with equivalent delivery rate on the right axis. The data shown are for GABA delivery.

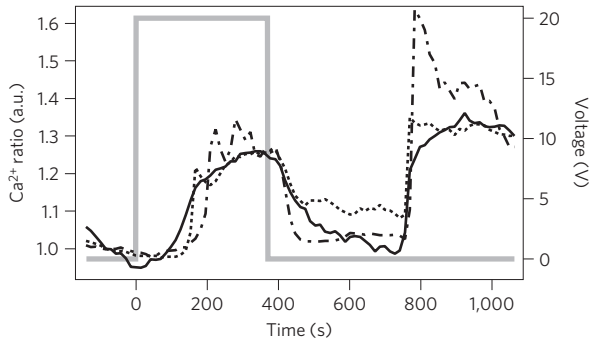

Figure 3 | Glu-induced Ca^{2+} responses in astrocytes. Time-lapse fluorescence microscopy of intracellular Ca^{2+} recordings in astrocytes induced by Glu delivered by the encapsulated device. Representative tracings from three cells (solid, dotted and dot–dash lines) in one experiment are shown. The device was switched on by application of voltage for 370 s (solid grey line) and then switched off. Cells were then allowed to re-establish their basal Ca^{2+} level. At 730 s, Glu was applied manually using a pipette ($[Glu]_{final} = 1$ mM), eliciting responses of similar magnitude to those from the device-delivered Glu. The experiment was repeated three times.

in intracellular Ca^{2+} revealed successful delivery of Glu (Fig. 3) after an equilibration delay similar to that observed in Fig. 2d. The Ca^{2+} response declined when the voltage was turned off and cells re-established their basal intracellular Ca^{2+} level. As a control, Glu was next applied manually using a pipette, resulting in a Ca^{2+} response of similar magnitude to that induced by Glu delivered from the encapsulated device. Collectively, this substantiates the usability of the device for cell activation, and that Glu retains its potent biological form after transport through the polymer.

Having demonstrated how this device converts electronic addressing signals into precise non-convective delivery of Glu, we next investigated its potential use as a novel communication interface between human-made electronics, selective neurotransmission and brain function. To test the feasibility of this concept, we used the auditory system of the guinea pig as an *in vivo* experimental platform. Within the cochlea, sound waves of various frequencies are transduced primarily by the inner hair cell system, as opposed to the outer hair cell system[30]. As Glu is the primary neurotransmitter for the inner hair cells, the auditory system can be used to evaluate the ability of the device to target specific cells, that is, whether the encapsulated ion pump can be used to selectively affect specific cell types *in vivo*. Excessive Glu is known to exert an excitotoxic effect on the inner hair cells as opposed to the outer hair cells[31,32], and this pathophysiological effect can be monitored by histological analysis. In addition, excitotoxicity can be analysed in real-time, by monitoring the auditory brainstem response (ABR). Excessive Glu will damage the inner hair cells, leading to hearing loss and an attenuated ABR. In the cochlea, high-frequency sound waves are transduced at the base, near the round window membrane (RWM), whereas lower frequencies are transduced towards the apex. Therefore, shifts in ABR threshold (re:pre-treatment threshold) at different frequencies indicate, in real-time, the effect of Glu at different distances up the cochlea. At present, osmotic pumps are used to modulate such effects by direct fluid injection[33]. However, the inner hair cells, positioned on a delicate membrane that vibrates with sound stimulation, are highly mechanosensitive, for example, to disturbances in fluid flow and pressure[34]. To bypass this problem, the ion pump can be used to deliver substances through the RWM, which is an established port of diffusive entry into the cochlea.

The tip of the delivery device was introduced in close proximity to the RWM of anaesthetized guinea pigs using conventional ontological surgery (Fig. 4a). The procedure is non-invasive to the cochlea, because the device delivers Glu to the outside of the RWM through which Glu enters by diffusion (Fig. 4b). Once the device was in place, Glu was delivered continuously for 60 min ($n = 5$) and during this time, ABR shifts were assessed at 0, 15, 30 and 60 min. Within this time frame, stimulation in the lower basal region (corresponding to 20 kHz transduction), upper basal region (16 kHz) and lower apical region (8 kHz) could be achieved without risking saturation of the entire cochlea with Glu. As the Glu solution

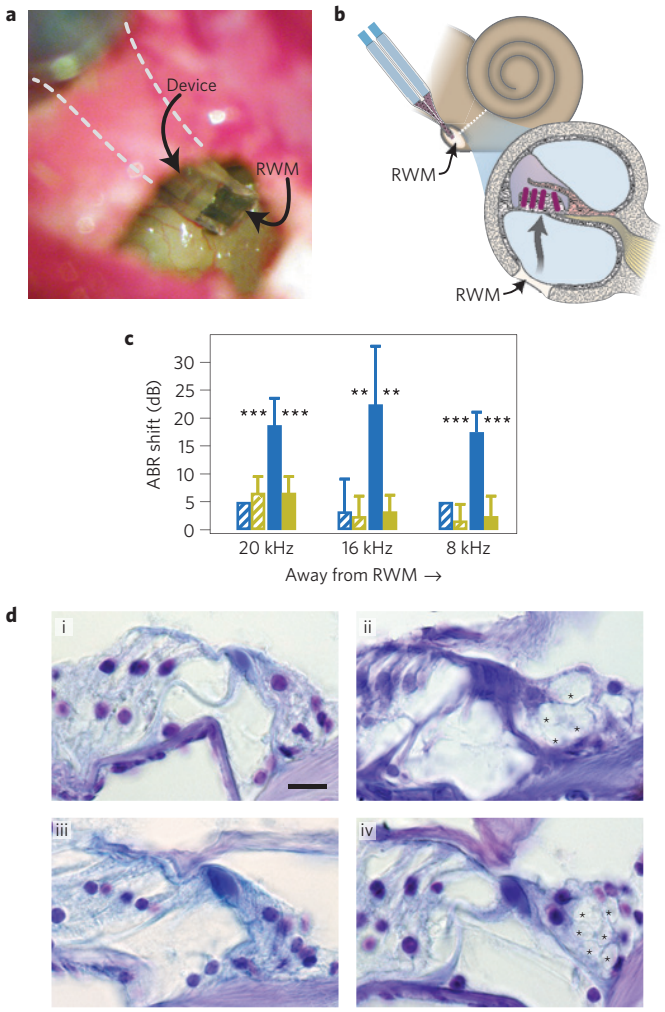

Figure 4 | *In vivo* application of the ion pump. a, Photograph of the device mounted on the RWM, with the two ion channels (see Fig. 1d) visible as dark blue strips on the transparent substrate. The dashed lines indicate the obscured shape of the device leading back to the electrolyte reservoirs, seen in the upper left of the image. **b**, Illustration of the experimental scheme. The dotted line indicates a slice through the cochlea, expanded below. The grey arrow indicates the diffusion of ions through the RWM, scala tympani and finally to the hair cells. **c**, Mean ABR shift (re:pre-treatment thresholds) as a function of recording frequency after 15 min (hatched bars) and 60 min (filled bars) of Glu (blue) and H^+ (yellow) delivery. The frequencies are illustrated in relation to their increasing distance from the RWM. The error bars indicate the standard deviation. **e**, Histological sections of the cochlea with the inner hair cells on the right and outer hair cells on the left showing (i) effect of H^+ delivery (as control) and (ii) effect of Glu delivery (excitotoxic-induced damage to the auditory dendrites indicated with asterisks) in the lower basal region (turn 1), and similar (iii) H^+ and (iv) Glu effect in the upper basal region (turn 2). Scale bar: 20 μm.

was at low pH, control experiments ($n = 3$) delivering only H^+ were also carried out. At 15 min, an ABR shift of only ~7.5 dB was observed for both Glu and H^+ for all frequencies, indicating that the Glu concentration had yet to reach excitotoxic levels (Fig. 4c). At the 30 min time point, increased ABR shifts (~10 dB, data not shown) were observed in some cases for Glu, whereas the H^+ response remained consistently low. After 60 min of Glu delivery, however, a strong, statistically significant ABR threshold shift (that is, hearing loss) was noted at all frequencies, whereas the H^+ response remained consistently low.

After the ABR recordings, cochleae were removed and prepared for histological analysis using cresyl violet (Fig. 4d). Control experiments revealed that delivered H^+ had little or no effect on any cell type. Similarly, no morphological changes were observed in the most apical regions of the cochlea after Glu was introduced into the perilymph (see Supplementary Fig. S1). However, in the lower and upper basal region, a strikingly large number of the dendrites of the inner, but not the outer hair cells, were observed to be swollen. As these dendrites represent the main connection between the inner hair cells and the underlying auditory nerves, the damaging, excitotoxic effect of Glu explains the corresponding ABR shifts at these frequencies. Collectively, these data indicate that the encapsulated ion pump can be used to establish concentration gradients within the perilymph, providing a means to spatially control excitotoxicity. Furthermore, this demonstrates that delivery of a particular neurotransmitter from the device can be used to selectively target a specific cell type *in vivo*, as responses are induced solely in the subset of cells expressing the relevant receptor.

Electronic control provides another highly desirable feature: the ability to expose cells to pulsed, rather than continuous delivery. Sustained exposure to neurotransmitters quickly desensitizes the receptors, reflected in, for example, malfunctioning signalling pathways or downregulation of receptor expression. Using pulsed delivery, such problems can be circumvented. In the present experiment, ~14 nmol of Glu was delivered during the 60 min 'pulse'. The device could accordingly be pulsed more than 100 times without depleting the ~30 μl Glu solution. Tailoring the pulsing scheme according to the physiological requirements could increase the effective lifetime even further.

Having demonstrated the ability to translate electronic addressing signals, through neurotransmitter signalling, into brainstem responses, this technology establishes a new paradigm in machine-to-brain interfacing. Indeed, the device described herein is the first successful realization of an organic electronic device capable of modulating mammalian sensory function by precise delivery of neurotransmitters. These developments represent a significant step forwards in biology–technology interfacing, and promise to pioneer further symbiosis of electronics and living systems.

Methods

Planar ion pump devices were fabricated using standard photolithographic methods as previously reported[18]. Briefly, prefabricated films of PEDOT:PSS on a polyethylene terephthalate substrate were dry-etched, selectively (by means of photolithographic masking) chemically over-oxidized and selectively (again by photolithographic masking) coated with the hydrophobic photoresist SU-8. After soaking in deionized water for >12 h, Glu, Asp and GABA were transported at various driving voltages between 2 and 10 V for a variety of times at each voltage from 0.1 M source electrolytes. Individual devices were used for each set of parameters. The transport was characterized in terms of the current versus time, as measured by the custom control electronics, and the quantity of the delivered molecules, as determined by quantitative HPLC analysis of the target electrolyte. Device efficiency was thus evaluated as the ratio of electrons passed through the driving circuitry to the number of molecules delivered to the target electrolyte.

Encapsulated ion pump devices were fabricated in a similar fashion as the planar devices. Devices were cut from the substrate using a computer-controlled flatbed cutting plotter, and sheathed with two pieces of silicone tubing each. The delivery-end of each tube was sealed and much of the length of the delivery 'tip' was covered with the ion-impermeable silicone encapsulant Sylgard 186 (Dow Corning).

For *in vitro* testing, primary murine astrocyte cultures were prepared and maintained as previously described[35], then loaded with the Ca^{2+}-sensitive dye FURA-2 AM. The encapsulated device was evaluated by delivering Glu and observing the subsequent fluxes in intracellular [Ca^{2+}] using ratiometric time-lapse fluorescence microscopy. As a control, Glu was also applied manually using a pipette to a final concentration of 1 mM.

For *in vivo* testing of the encapsulated device, access to the RWM of the anaesthetized guinea pig was achieved by a retro-auricle approach. Once the device was placed on the RWM, delivery using either 0.1 M L-glutamic acid in 10 μM HCl(aq) (pH ~ 3) as the source electrolyte and 0.1 M NaCl(aq) as the cathodic electrolyte was initiated. Control experiments delivering H^+ used 0.1 M HCl(aq) (pH 1) as the source electrolyte. Over a 60 min time frame, auditory function was assessed by means of auditory brainstem response at frequencies of 8, 16 and

20 kHz at 0, 15, 30 and 60 min time points. Afterwards, cochleae were collected for histological analysis and stained with cresyl violet.

Full methods are available in Supplementary Methods.

Received 24 February 2009; accepted 2 June 2009; published online 5 July 2009

References

1. Wilson, B. S. *et al.* Better speech recognition with cochlear implants. *Nature* **352,** 236–238 (1991).
2. Kumar, R. *et al.* Double-blind evaluation of subthalamic nucleus deep brain stimulation in advanced Parkinson's disease. *Neurology* **51,** 850–855 (1998).
3. Mayberg, H. *et al.* Deep brain stimulation for treatment-resistant depression. *Neuron* **45,** 651–660 (2005).
4. Hochberg, L. R. *et al.* Neuronal ensemble control of prosthetic devices by a human with tetraplegia. *Nature* **442,** 164–171 (2006).
5. George, P. *et al.* Fabrication and biocompatibility of polypyrrole implants suitable for neural prosthetics. *Biomaterials* **26,** 3511–3519 (2005).
6. Williams, J. C., Holecko, M. M., Massia, S. P., Rousche, P. & Kipke, D. R. Multi-site incorporation of bioactive matrices into MEMS-based neural probes. *J. Neural Eng.* **2,** L23–L28 (2005).
7. Richardson-Burns, S. *et al.* Polymerization of the conducting polymer poly(3,4-ethylenedioxythiophene) (PEDOT) around living neural cells. *Biomaterials* **28,** 1539–1552 (2007).
8. Green, R., Lovell, N., Wallace, G. & Poolewarren, L. Conducting polymers for neural interfaces: Challenges in developing an effective long-term implant. *Biomaterials* **29,** 3393–3399 (2008).
9. Abhyankar, V., Lokuta, M., Huttenlocher, A. & Beebe, D. Characterization of a membrane-based gradient generator for use in cell-signalling studies. *Lab Chip* **6,** 389–393 (2006).
10. Guimard, N., Gomez, N. & Schmidt, C. Conducting polymers in biomedical engineering. *Prog. Polym. Sci.* **32,** 876–921 (2007).
11. Hendricks, J., Chikar, J., Crumling, M., Raphael, Y. & Martin, D. Localized cell and drug delivery for auditory prostheses. *Hear. Res.* **242,** 117–131 (2008).
12. Xu, H., Wang, C., Wang, C., Zoval, J. & Madou, M. Polymer actuator valves toward controlled drug delivery application. *Biosens. Bioelectron.* **21,** 2094–2099 (2006).
13. Zinger, B. & Miller, L. L. Timed release of chemicals from polypyrrole films. *J. Am. Chem. Soc.* **106,** 6861–6863 (1984).
14. Pernaut, J. & Reynolds, J. R. Use of conducting electroactive polymers for drug delivery and sensing of bioactive molecules. A redox chemistry approach. *J. Phys. Chem. B* **104,** 4080–4090 (2000).
15. Abidian, M. R., Kim, D. & Martin, D. C. Conducting-polymer nanotubes for controlled drug release. *Adv. Mater.* **18,** 405–409 (2006).
16. Pei, Q. & Inganaes, O. Electrochemical applications of the bending beam method. 1. Mass transport and volume changes in polypyrrole during redox. *J. Phys. Chem.* **96,** 10507–10514 (1992).
17. Wang, X., Shapiro, B. & Smela, E. Visualizing ion currents in conjugated polymers. *Adv. Mater.* **16,** 1605–1609 (2004).
18. Isaksson, J. *et al.* Electronic control of Ca^{2+} signalling in neuronal cells using an organic electronic ion pump. *Nature Mater.* **6,** 673–679 (2007).
19. Chiang, C. *et al.* Electrical conductivity in doped polyacetylene. *Phys. Rev. Lett.* **39,** 1098–1101 (1977).
20. Heywang, G. & Jonas, F. Poly(alkylenedioxythiophene)s—new, very stable conducting polymers. *Adv. Mater.* **4,** 116–118 (1992).
21. Groenendaal, L., Jonas, F., Freitag, D., Pielartzik, H. & Reynolds, J. R. Poly(3,4-ethylenedioxythiophene) and its derivatives: Past, present, and future. *Adv. Mater.* **12,** 481–494 (2000).
22. Zhu, Z. *et al.* A simple poly(3,4-ethylene dioxythiophene)/poly(styrene sulfonic acid) transistor for glucose sensing at neutral pH. *Chem. Commun.* 1556–1557 (2004).
23. Isaksson, J. *et al.* Electronically controlled pH gradients and proton oscillations. *Org. Electron.* **9,** 303–309 (2008).
24. Riedel, G., Platta, B. & Micheau, J. Glutamate receptor function in learning and memory. *Behav. Brain Res.* **140,** 1–47 (2003).
25. Cryan, J. & Kaupmann, K. Don't worry 'B' happy!: A role for $GABA_B$ receptors in anxiety and depression. *Trends Pharmacol. Sci.* **26,** 36–43 (2005).
26. Meldrum, B. S. Glutamate as a neurotransmitter in the brain: Review of physiology and pathology 1. *J. Nutr.* **130,** 1007S–1015S (2000).
27. Sontheimer, H., Kettenmann, H., Backus, K. H. & Schachner, M. Glutamate opens Na^+/K^+ channels in cultured astrocytes. *Glia* **1,** 328–336 (1988).
28. Usowicz, M. M., Gallo, V. & Cull-Candy, S. G. Multiple conductance channels in type-2 cerebellar astrocytes activated by excitatory amino acids. *Nature* **339,** 380–383 (1989).
29. Glaum, S. R., Holzwarth, J. A. & Miller, R. J. Glutamate receptors activate Ca^{2+} mobilization and Ca^{2+} influx into astrocytes. *Proc. Natl Acad. Sci. USA* **87,** 3454–3458 (1990).
30. Purves, D. (ed.) *Neuroscience* 4th edn 283–314 (Sinauer, 2004).
31. Pujol, R., Lenoir, M., Robertson, D., Eybalin, M. & Johnstone, B. Kainic acid selectively alters auditory dendrites connected with cochlear inner hair cells. *Hear. Res.* **18,** 145–151 (1985).
32. Duan, M., Agerman, K., Ernfors, P. & Canlon, B. Complementary roles of neurotrophin 3 and a N-methyl-d-aspartate antagonist in the protection of noise and aminoglycoside-induced ototoxicity. *Proc. Natl Acad. Sci. USA* **97,** 7597–7602 (2000).
33. Bianchi, L. & Raz, Y. Methods for providing therapeutic agents to treat damaged spiral ganglion neurons. *Curr. Drug Targets: CNS Neurol. Disord.* **3,** 195–199 (2004).
34. Ohyama, K., Salt, A. & Thalmann, R. Volume flow rate of perilymph in the guinea-pig cochlea. *Hear. Res.* **35,** 119–129 (1988).
35. Dobrenis, K. Microglia in cell culture and in transplantation therapy for central nervous system disease. *Methods* **16,** 320–344 (1998).

Acknowledgements

We wish to thank S. Plantman for providing primary astrocyte cultures, J. Kehr for access to the HPLC equipment, A. Viberg for technical assistance and D. Nilsson, P. Kjäll and T. Nakagawa for valuable discussion. This project has been carried out within the Strategic Research Center for Organic Bioelectronics (OBOE, www.oboe.nu) funded by the Swedish Foundation for Strategic Research (SSF). The Organic Electronics Group at Linköping University in Norrköping is a member of the COE@COIN project, also funded by the SSF. B.C. is supported by the Swedish Research Council, Funds of Karolinska Institutet and Tysta Skolan. The agencies that have supported this study were not involved in the design, interpretation, analysis or review of the data.

Author contributions

D.T.S. was responsible for the design, characterization and operation of the encapsulated device, and primary preparation of the manuscript. S.K. characterized the planar devices and K.C.L. carried out *in vitro* cell experiments and assisted with operation of the devices *in vivo*. R.H. and B.C. carried out the surgical procedure and subsequent audiological and physiological analysis. K.T. manufactured the planar devices, M.G. carried out HPLC analysis and both K.T. and E.W.H.J. aided in the design of the encapsulated device. M.B., B.C. and A.R.-D. are the senior authors of the paper. Each was responsible for supervision in their respective departments, as well as project planning and preparation of the manuscript.

Additional information

Supplementary information accompanies this paper on www.nature.com/naturematerials. Reprints and permissions information is available online at http://npg.nature.com/reprintsandpermissions. Correspondence and requests for materials should be addressed to A.R.-D.